Next-Generation Custom-Fit Reusable Respiratory Protective Device with Continuous Fit Monitoring – Part III: 3D Printing of Prototypes and Evaluation

Sungmee Park[1], Yuanqing Tian[2], Michael Bergman[3], Jonisha Pollard[3], Ziqing Zhuang[3], and Sundaresan Jayaraman[1*]

[1] Georgia Institute of Technology, School of Materials Science and Engineering

[2] Georgia Institute of Technology, School of Industrial Design

[3] National Institute for Occupational Safety and Health, National Personal Protective Technology Laboratory

*Corresponding author: Sundaresan Jayaraman, sundaresan.jayaraman@gatech.edu, Phone: 404.894.2461

ABSTRACT

Some respiratory protective devices (RPDs) such as filtering facepiece respirators (FFRs) are manufactured in discrete sizes, with some models being limited in accommodating the fit of some gender and race combinations. This study presents the development of a custom-fit RPD which conforms to a user's facial features and flexes and moves with facial movements during use. Our design also integrates a pressure-sensing network, which continuously monitors fit and will alert the user when the fit is compromised.

In this final part of the three-part series, we transform the digital prototypes of the custom-fit RPD presented in Parts I and II to physical prototypes through 3D printing (additive manufacturing) using silicone-based elastomers. We identify the key material properties required for creating the physical prototypes. Based on a comparative analysis of commercially available materials, we select two of them and create prototypes of the RPD using two different commercial 3D printers. We then demonstrate the responsiveness of the custom-fit RPD to changes in facial profile during use from natural (neutral facial expression with mouth closed) to talking, to smiling, and to yawning, and the quantification of the changes in pressure at the faceseal by the continuous fit monitoring system through an App running on an Android tablet. With the realization of the successful custom-fit RPDs using the developed methodology, we lay the foundation for providing respiratory protection, and improved source control, to the full spectrum of individuals in the United States public including children, for whom FFRs options are currently limited.

Keywords: Custom-fit respiratory protective device; continuous fit monitoring; 3D printing; additive manufacturing, Shore hardness; protection; comfort; faceseal pressure; pressure injury; data analytics; facial profile

INTRODUCTION

In Parts I and II of the three-part series (Park 2024a, Park 2024b), we established the need for a custom-fit respiratory protective device (RPD) with continuous monitoring of the fit of the device to enhance its role in protecting users from inhalation hazards in an effective manner during its use. We also created digital prototypes of the technology building blocks of the RPD. The primary objective of the research presented in this paper is to transform the digital prototypes into physical prototypes through additive manufacturing and carry out tests on the custom-fit RPD with the integrated continuous fit monitoring system to demonstrate the realization of the overall goals of the study. Specifically, the objective is to identify the characteristics required of the material for creating a custom-fit RPD so that it is shape-conformable, flexible, strong, and durable; then, use these requirements to select materials that are also processable in additive manufacturing to create the physical prototypes. Yet another objective is to integrate the continuous fit monitoring system into the RPD frame and test the App. The final objective is to demonstrate the responsiveness of the custom-fit RPD to changes in facial profile from natural (neutral facial expression with mouth closed) to talking, to smiling, and to yawning, and the quantification of the changes in pressure at the faceseal by the continuous fit monitoring system through the App.

METHODS

We now discuss the steps to transform the digital prototypes into physical prototypes through additive manufacturing (3D printing).

Material Evaluation and Selection

The material used to create the RPD frame must effectively balance device fit (protection) with comfort. It must be shape-conformable and ensure the frame's structural integrity over repeated use and decontamination. In addition, the materials must be 3D-printable. Therefore, the next step was to identify the key mechanical properties of materials that would meet the performance requirements of the RPD frame in terms of having the right combination of strength and flexibility that comes close to having the feel, softness, and flexibility of human skin. The Young's modulus of a material is the ratio of the stress to the strain in the elastic range of the material (Wiley 2024). Thus, it is a measure of the stiffness of the material and affects the shape-conformability of the RPD frame. The tensile strength of the material affects the strength of the RPD frame. The elongation at break of the material affects the stretchability of the RPD frame since it must respond to changes in the facial profile of the user when using the RPD. The tear strength of the material is another mechanical property of the material that affects the structural integrity of the RPD frame. As the Young's modulus of a material increases, its stiffness increases along with its tensile strength. However, its elongation will decrease. For a given design of the RPD frame, the density of the material will affect its weight, which, in turn, would affect the user's comfort when wearing it, especially for long durations. Therefore, these material properties and their inter-relationships were considered in the selection of materials for the RPD frame.

Figure 1 shows an Ashby plot of the relationship between density and Young's modulus of various classes of materials (Granta, 2020). It also shows the relationship between Young's modulus and tensile strength (Ashby, 2008).

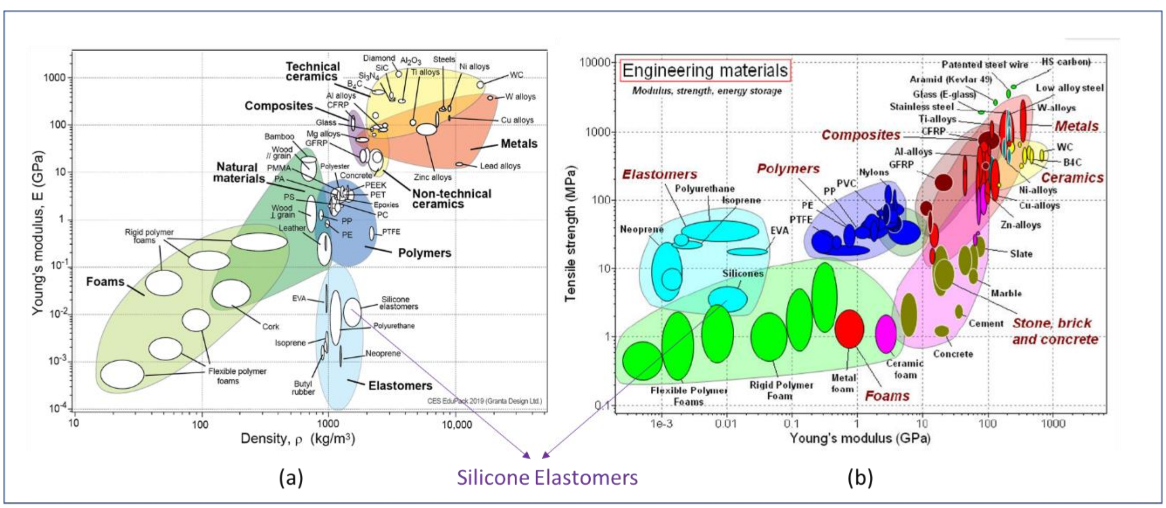

Figure 1. Ashby's Materials Property Charts. (a) Density versus Young's Modulus, (Granta, 2020). Chart created using CES EduPack2019, ANSYS Granta, © Granta Design. (b) Young's Modulus versus Tensile Strength, (Ashby, 2008).

As seen in the figure, elastomers is the class of materials with the right combination of strength and flexibility that comes close to having the feel, softness, and flexibility of human skin. These characteristics are important for the RPD since its usage over long durations should not cause pressure injuries. The materials in this class include ethyl-vinyl acetate, silicones, polyurethanes, and neoprene, among others. Furthermore, silicones fall into the class of flexible polymer foams, potentially making them ideal candidates for the RPD frame material.

Hardness is another important material property that should be considered in balancing comfort with fit, and hence protection. Figure 2 shows the Shore hardness continuum for the various classes of materials (Smooth-On, 2020). The chosen material should be in the range of extra-soft and soft materials with a maximum Shore hardness of 00-60, but preferably up to 00-40.

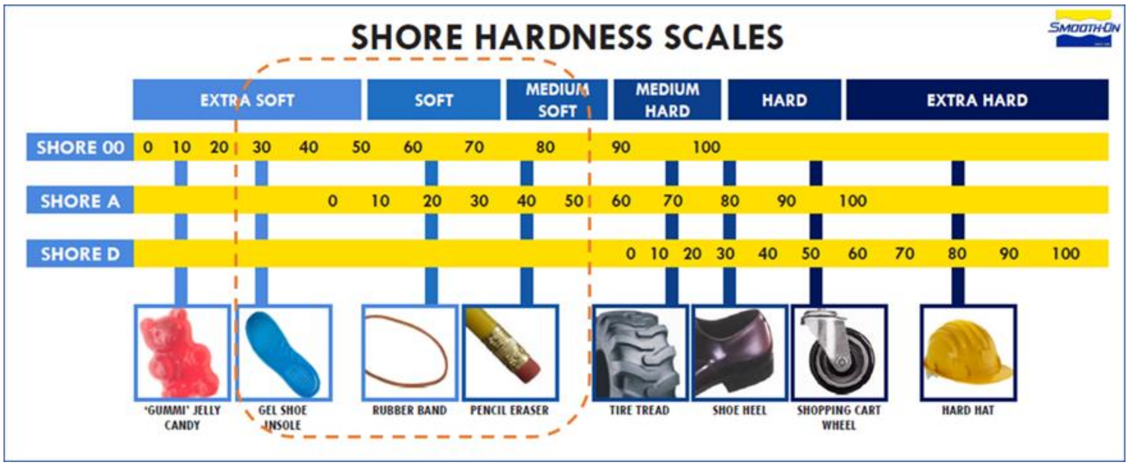

Figure 2. Shore Hardness Scales (Smooth-On, 2020). © Smooth-On, Inc.

Assessment of Commercial Materials: Table I shows the important properties of silicone-based materials from four major companies: Elastic 50A (Formlabs, 2022a), SIL30 (Carbon 3D, 2022), SILASTIC 3D 3335 LSR (Dow, 2022), and AMSil (Elkem, 2022).

Table I. Properties of Silicone-based Materials for 3D Printing

Company	Material	Tensile Strength	Tear Strength	Elongation @ Break	Shore Hardness	Material Type
		MPa	kN/m	%	A Class	
Formlabs	Elastic 50A	3.23	19.1	160	50	Silicone Urethane Elastomer
Carbon 3D	SIL 30	3.5	10	350	30	Silicone Urethane Elastomer
DOW	SILASTIC 3D 3335LSR	8.3	0.05	5.25	50	Liquid Silicone Rubber
Elkem	AMSil	2	10	200	70	Engineering Silicone

In evaluating the materials, Shore hardness is the most important property because the RPD must be soft on the user's face. After a comparative analysis of the properties, we decided on Elastic 50A and SIL 30 as potential candidates for creating the physical prototypes because their Shore A hardness was in the 30-50 range. As shown in Figure 2, any material with a Shore A hardness greater than 50 would feel like rubbing the face on a tire tread or harsher, which would not be comfortable since the RPD will be worn for long durations. Even though the Shore A hardness of Silastic from Dow was 50, its tear strength was only 0.05kN/m, which was very low compared to the other two materials. The low tear strength may cause the RPD frame to get damaged easily during use and therefore it was not chosen.

The tensile strength and elongation at break are the other two important mechanical properties since they influence the behavior of the RPD frame during use. The RPD frame must be strong enough to withstand constant handling and multiple uses over its lifetime, and this is determined by its tensile strength. While being strong, the RPD frame must "stretch" and respond to changes in facial profile during its use, which is determined by the material's elongation at break. As shown in the table, both SIL 30 and Elastic 50A have high elongations at break and tensile strength, rendering them suitable for the RPD frame.

Prior to producing the physical prototypes of the RPD frame, it was important to gauge the anticipated performance of the chosen materials (SIL 30 and Elastic 50A) for the RPD frame in the field. For this purpose, we used the properties of the materials used in elastomeric half-mask respirators (EHMR) as a benchmark since EHMRs are reusable and durable. The elastomers used in the construction of EHMRs include silicone, neoprene, and ethylene propylene diene monomer (EPDM) rubber (National Academies of Sciences, Engineering, and Medicine, 2019). These materials are also seen in Figure 1.

Table II shows the properties of thermoplastic elastomer (TPE) and silicone rubber used in manufacturing EHMRs. A comparison of the properties of the materials in Table 1 with those in Table 2 shows that the properties of the chosen materials for the RPD frame are within the range of those of the materials used for EHMRs. Therefore, the performance of the RPD frame in the field is expected, at the very minimum, to be in line with that of EHMRs. Studies to assess the durability of the custom-fit RPD from a materials standpoint will form the basis of future research.

Table II. Properties of Materials Used in EHMRs

Material	Tensile Strength	Tear Strength	Elongation @ Break	Shore Hardness
	MPa	kN/m	%	A Class
Thermoplastic Elastomer	0.255 - 51.0	1.60 - 275	9.50 - 1660 %	2 – 98
Silicone Rubber	0.138 - 165	0.877 - 182	5.00 - 1490 %	1 - 95

Sources: Thermoplastic Elastomer, Matweb, 2024a; Silicone Rubber: Matweb, 2024b.

Both SIL 30 and Elastic 50A can be decontaminated after use with UV radiation or other cleaning solvents including bleach (NaClO, 5%), sanitizer (NH_4Cl, 10%), and cleaning solvents or disinfectants for elastomeric respirators (Carbon3D, 2024).

Printing Physical Prototypes from Digital Frames

We printed the Base Frame and Covering Piece designs first using PLA (Polylactic Acid) on an FDM (fused deposition modeling) printer to ensure their printability and to identify any potential flaws in the design or the specifications. Once the physical prototypes matched the digital specifications, we printed them using Elastic 50A on Form 3 printers from Formlabs (Form 3, Somerville, MA, USA) in the Invention Studio at Georgia Tech and using SIL 30 on M2 printers at Carbon 3D (M2, Redwood City, CA, USA). The weight of the RPD frame (Base Frame + Covering Piece) printed using SIL 30 and Elastic 50A was 48 grams. The facepiece of a typical EHMR weighs 82 grams (3M, 2024).

Since the Fastening Hub will be mounted on the user's head, it must conform to the shape of the head while simultaneously being soft on the head and strong. Unlike the Base Frame and Covering Piece in the RPD, which are moving constantly since the facial profile of the user changes during typical use (e.g., talking and smiling), the hub on the head does not move once it is donned. However, it must be strong enough to withstand the stress experienced during donning and doffing. For this reason, we chose Elastic 80A from Formlabs for printing the Fastening Hub on Form 3 (Formlabs, 2022b). Its tensile strength is 8.9MPa, tear strength is 24kN/m, elongation at break is 120%, and has a Shore A Hardness of 80. The weight of the Fastening Hub was 142 grams (solid piece) and 84 grams with Voronoi tessellations. The screw sets were printed using PLA on an FDM printer. Figure 3 shows the physical prototype produced using SIL 30 on a headform.

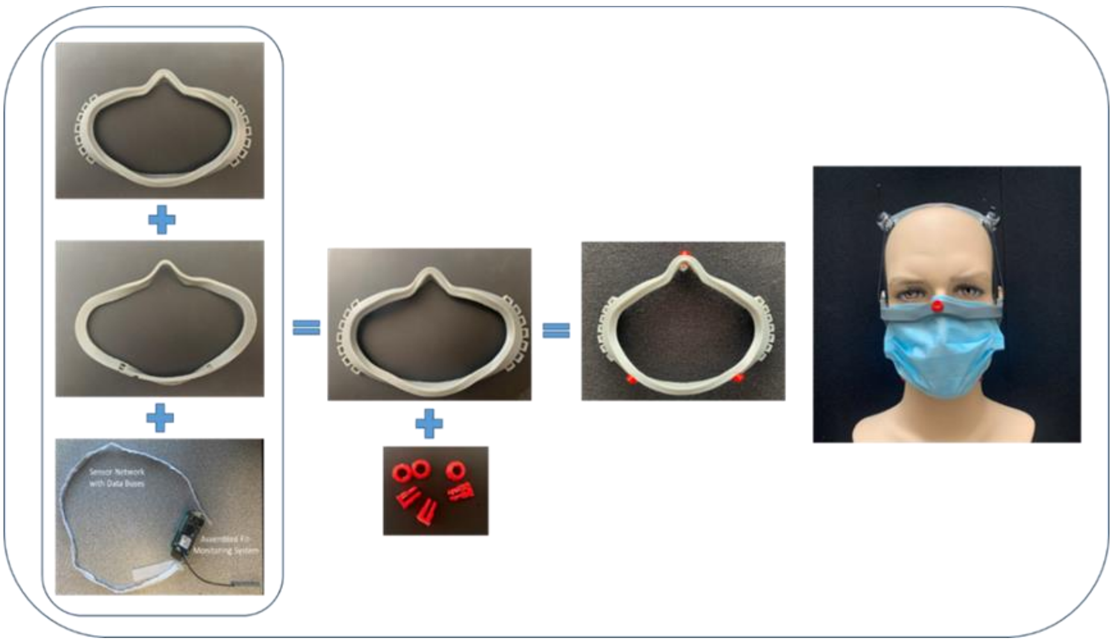

Figure 3. Bringing it Together: The Custom-Fit RPD on a Headform.

By way of the above process, the concept of scanning and digitizing an individual's facial profile and creating a custom-fit respiratory protective device with continuous fit monitoring has been realized successfully.

RESULTS AND DISCUSSION

We now discuss the testing of the continuous fit monitoring App followed by the testing of the total custom-fit RPD with integrated continuous fit monitoring.

Testing the Continuous Fit Monitoring App

Figure 4 shows the user dashboard in the App running on an Android tablet along with the visualization of the pressure heat map. The menu options shown on the left in the dashboard include View Visualizations, View Pending Alerts, View History of Alerts, View Profile, and Logout. The View Visualizations option displays the color-coded heat map to reflect the magnitude of the pressure under each sensor. The color thresholds for the heat map can be configured in the App to suit the requirements. In the figure, the ADC (analog to digital) values are displayed. When the option to display the pressure in lb/in^2 is chosen in the App, the pressure will be displayed in lb/in^2.

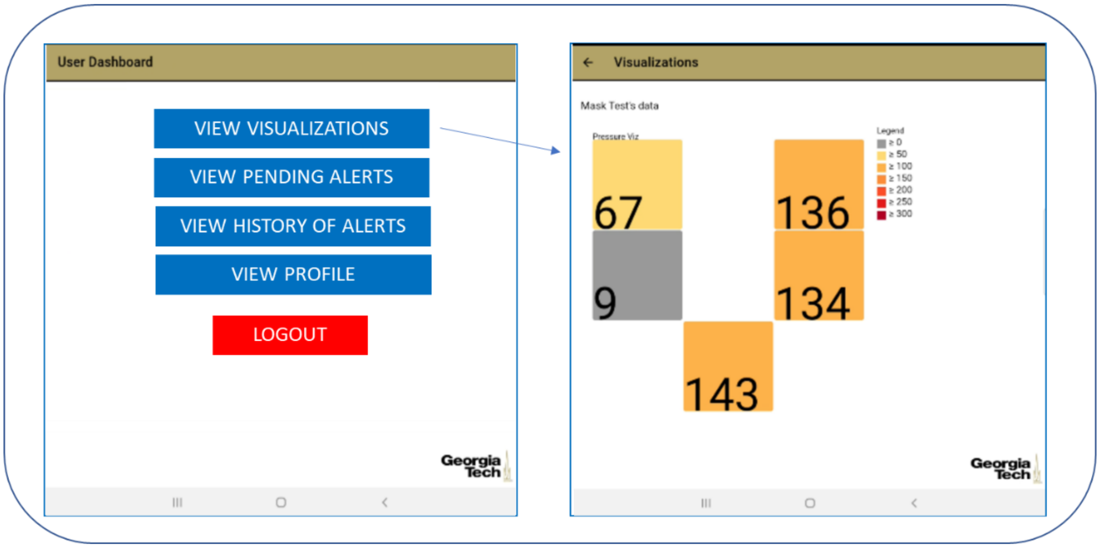

Figure 4. User Dashboard and Pressure Heat Map Visualization in the App

When the faceseal pressure falls below a certain threshold under one of the sensors, an alert is sent to the user's App on the device with a message to adjust/tighten the RPD. Those alerts are stored under "Pending Alerts," implying that the potential for a faceseal leakage is high unless the user corrects the position of the RPD. When the user adjusts the RPD, the system detects the change in pressure. If it meets the defined threshold, the alert is removed from Pending Alerts and stored in "History of Alerts." These alerts can be analyzed at a later date to understand the performance of RPD over time and to spot any specific trends or activities during use that lead to faceseal leakage. This type of data analytics, facilitated by the unobtrusive means to monitor pressure data in real time, will be valuable in enhancing the design of RPDs. The "User Profile" option in the menu is used to enter information about the user, which can then be correlated with other data to enhance personalization of the device.

Figure 5 shows the sequence of operations during the typical use of the custom-fit RPD with integrated continuous fit monitoring.

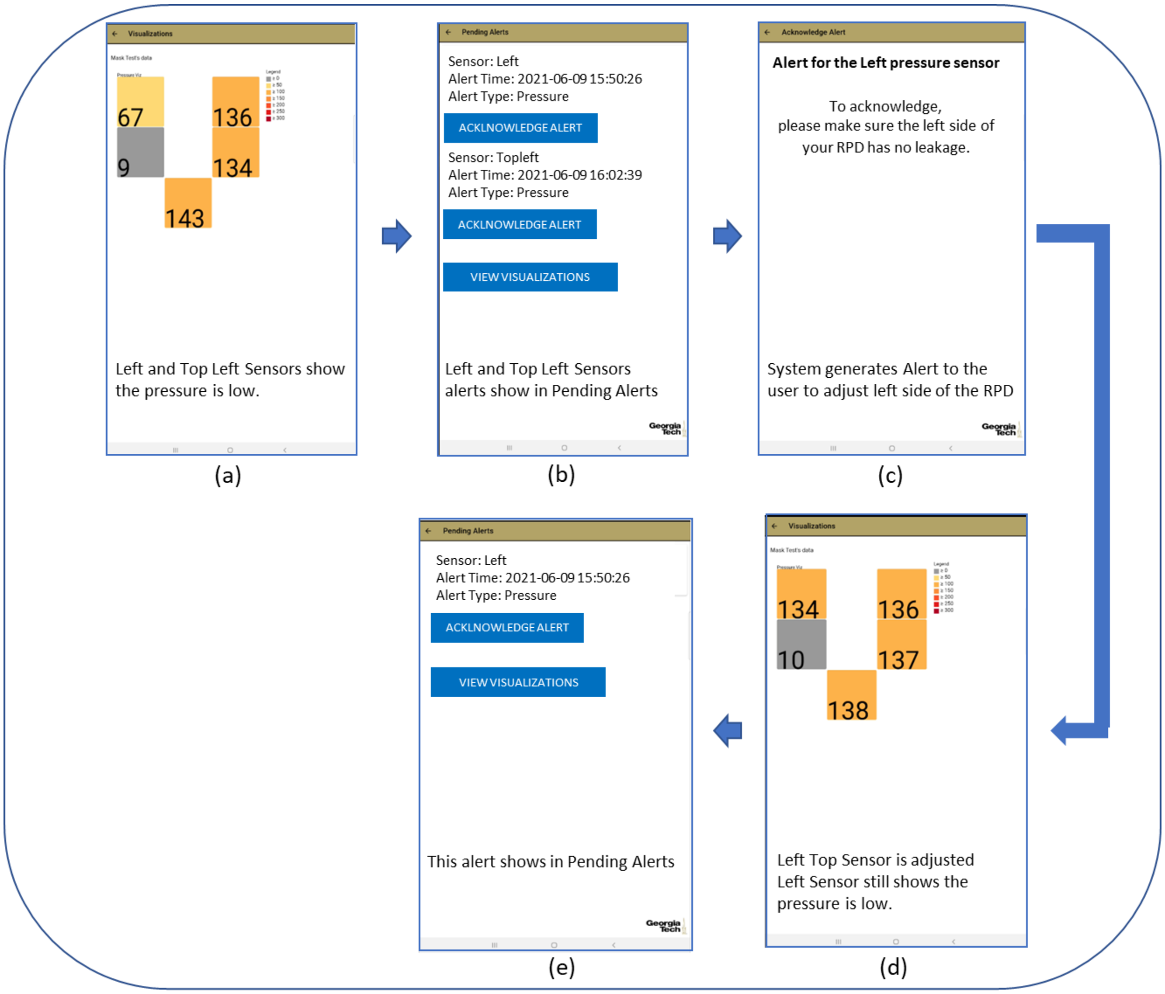

Figure 5. Flow of Actions in the Continuous Fit Monitoring System App. (a) Heat Map displays pressure distribution. (b) Pending Alerts: Lists the sensors with low pressure (left and top left). (c) Alert generated for user to adjust RPD. (d) RPD adjusted by user: Pressure in top left sensor increases. (e) Pending Alerts: Continues to list left sensor.

When the user chooses the “View Visualizations” option in the main menu, the pressure heat map is displayed as shown in Figure 5(a). Since the top left and left sensors are below the threshold value set in the App, it generates two alerts to the user indicating areas of potential faceseal leakage. When the “View Pending Alerts” option is chosen, the two alerts are displayed as in Figure 5(b). Figure 5(c) shows the alert to the user, suggesting the adjustment of the RPD. When the user adjusts the RPD, the pressure in the top left sensor goes above the set threshold as shown in Figure 5(d), and that alert is moved to “History of Alerts.” However, the user has not adjusted the RPD in the area under the left sensor; therefore, the alert for the left sensor remains as shown in Pending Alerts in Figure 5(e).

All the pressure values, alerts, and actions are stored in the database and can be retrieved for carrying out data analytics to understand the performance of the RPD over time. The data can also be used to identify the potential for a pressure injury from donning the RPD for long periods of time and alerting the user to prevent a pressure injury. In short, the developed custom-fit RPD with the integrated continuous fit monitoring system can become an unobtrusive data acquisition platform for research and development of RPDs, including human factors associated with the use of RPDs both in real time and over time in workplaces with inhalation hazards.

Total System Testing

Once the App was tested successfully, we carried out a series of tests to evaluate the responsiveness of the RPD to changes in facial profile and quantification of the resulting changes in the pressure at the faceseal. The results presented here are from the tests carried out on one of the three participants in the study. The RPD was connected to the Fastening Hub using a set of straps. As the straps were tightened and loosened, the pressure at the faceseal changed. These changes were reflected in the pressure values sensed by the network and displayed in the heat map in the App, thus demonstrating the responsiveness of the sensor network and the successful operation of the App. In practice, the “optimum” or baseline pressure at the faceseal to ensure proper fit will be established during the very first donning or the calibration phase of the RPD at the time of issuance of the RPD when a QNFT is performed. The design of the system with the multiple fastening hooks, straps, and the fastening hub will enable the user to customize and set the "ideal" pressure configuration so that they are both comfortable and protected against the inhalation hazard by passing the QNFT. This will also prevent them from tightening the RPD excessively resulting in pressures in excess of the ideal pressures needed to pass the fit test, which could then lead to pressure injuries, especially when the RPD is worn over long durations. The positions of the straps can be marked to ensure the right fit, and facilitate quick and correct donning during repetitive use. When the RPD is used, the pressures at the five sensors in the faceseal are monitored continuously in real-time. The built-in algorithm in the App compares the baseline values with the sensed pressures and determines the potential for a faceseal leakage (based on a defined threshold customized for the user). Depending on the result of this assessment, the App might issue an alert to the user to adjust the frame to prevent leakage and ensure protection against the inhalation hazard.

Figure 6 shows the ADC values displayed in the App, which correspond to the pressures in the five sensors prior to donning by the participant. When the pressure is measured in lb/in^2, the change in the pressure value at the sensors at the faceseal due to facial movement will be small. Therefore, we use ADC values to demonstrate the responsiveness of the sensor network to small changes in pressure with facial movement.

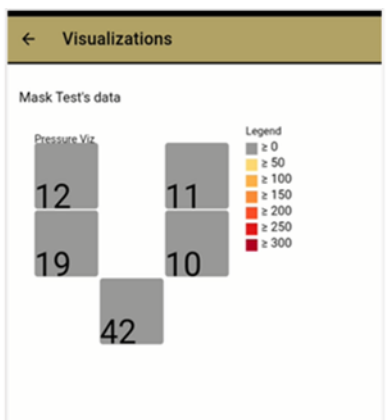

Figure 6. Heat Map with ADC Values in the Continuous Fit Monitoring System App

We tested the effect of changes in facial profile – from natural (neutral facial position with lips closed) to talking to smiling and to yawning – on the pressure distribution in the faceseal on Subject A. Figure 7 shows a composite view of the digital scans of the facial profiles of the participant in the four states. The degrees of movement of the key landmarks, Chin (2), Jaw Side Point (D2) and Face Side Point (D3), and the contours of the RPD Frame are shown as solid lines in different colors with changes in facial profiles. For developing these contours, we followed the steps that were similar to those followed for FFRs and described in relation to Figure 1 of Part II. Here, we used the custom-fit RPDs during scanning (instead of the FFRs in Part II) for assessing the degrees of movement for the chosen landmarks for the three individuals and developed the contours shown in the different colors for the four states. In Figure 7, the red color represents the natural state. The other colors – blue, green, and orange – show how the profile changes correspondingly with talking, smiling, and yawning. The contour line with the key landmarks in each state is also shown in that color. For the talking, smiling, and yawning states, we also show the natural state (in red) as the "base" to facilitate easy comparison of the degree of movement of the landmarks, which corresponds to the movement of the RPD frame. The figure also shows the corresponding pressure heat map for each state.

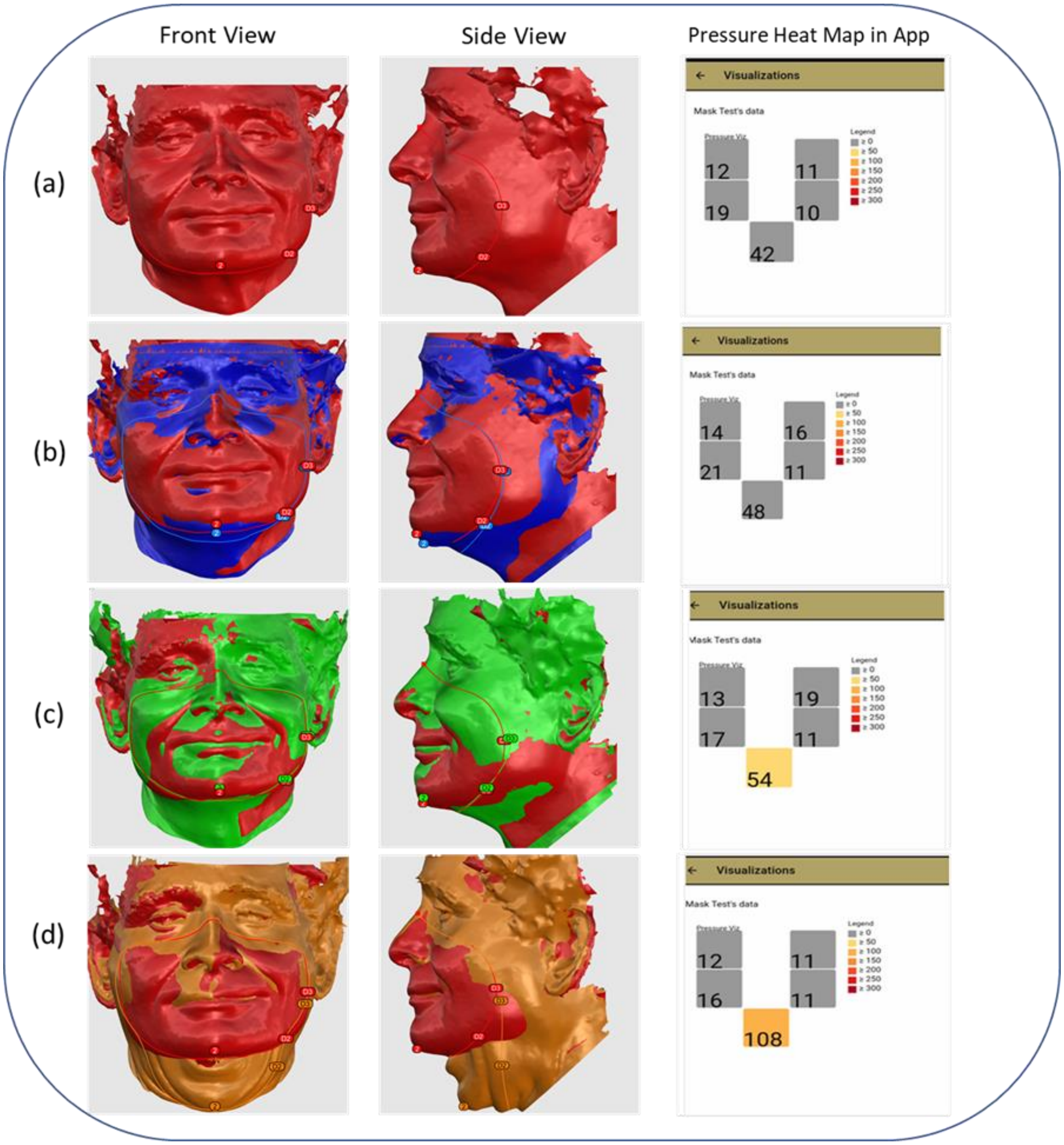

Figure 7. Custom-fit RPD on One Participant: Front and Side Views, Landmarks, RPD Frame Contours, and Pressure Distribution in Four States. (a) Natural State; (b) Natural and Talking; (c) Natural and Smiling; (d) Natural and Yawning.

In Figure 7(a), which corresponds to the participant's natural state, the pressure in the chin sensor is greater when compared to that in Figure 6. In the talking state in Figure 7(b), the pressure is higher in all the sensors. These changes in pressure values are also reflected in the degree of movement of the three landmarks from the natural to the talking state shown in the facial profiles in the figure. The solid red and blue lines represent the contours of the RPD Frame in the natural and talking states, respectively. This confirms that the RPD responds to changes in the facial profile and moves with the landmarks, which is essential for ensuring the integrity of the faceseal.

In the smiling state in Figure 7(c), there is a change in the pressure values from the talking state, albeit by a small amount. These changes in pressure values are also reflected in the degrees of movement of the landmarks from the natural to the smiling state shown in the figure. The contours of RPD Frame in the natural and smiling states are also shown in the figure in the solid red and green lines, respectively. This once again confirms that the RPD responds to changes in the facial profile and moves with the landmarks, which is essential for ensuring the integrity of the faceseal.

In the yawning state in Figure 7(d), the pressure has increased significantly in the chin sensor. This significant change in pressure value is also reflected in the degrees of movement of the landmarks from the natural to the yawning state shown in the figure. The contours of the RPD Frame in the natural and yawning states are also shown in the figure in the solid red and orange lines, respectively. This once again confirms that the RPD responds to changes in the facial profile and moves with the landmarks, which is essential for ensuring the integrity of the faceseal. The responses of the RPD frame to changes in facial profiles for the other two participants were similar.

In sum, this series of tests demonstrates the responsiveness of the custom-fit RPD to changes in facial profile and the quantification of the changes in pressure at the faceseal by the continuous fit monitoring system through the App running on an Android tablet.

Limitations of the study

In addition to the limitations of the study mentioned in Parts I and II, the economics associated with the use of the novel RPD with continuous fit monitoring have not been analyzed. This will be a subject of future research. The important issues related to regulatory compliance for use in workplaces have not been considered here and must be investigated for the implementation of the technology. The three individuals participating in the study were adults. Extensive field-testing on a larger population to assess the relative accuracy, precision, and reliability of the sensor network is outside the scope of the work presented here and will be a topic of future research. Likewise, factors related to the durability of the materials used in producing the custom-fit RPDs during repeated use have not been assessed. Since the facial profiles of these individuals were different, it is anticipated that the algorithms should be applicable to children as well; however, the algorithms have not been experimentally applied to children to create customized RPD frames with continuous fit monitoring, which will be a topic of future research.

CONCLUSIONS

We have demonstrated the successful application of the structured design methodology through the realization of the physical prototypes of the custom-fit RPD with fit monitoring for three individuals from the digital prototypes generated using the taxonomy of landmarks. We also demonstrated the responsiveness of the physical prototypes of the custom-fit RPD to changes in facial profile during use by following the movement of the chosen landmarks that defined the contour of the frames during their design. This responsiveness or degree of movement of the custom-fit RPDs to changes in facial profiles during the four stages also validates the choice of materials used in producing them.

Through this series of three papers, we have demonstrated the workflow leading to the successful design, development, and testing of a custom-fit reusable RPD comprising the technology building blocks of a Base Frame, a Covering Piece, a Fastening Hub, and a continuous fit monitoring system. However, the actual respiratory protection provided by the custom-fit RPD against inhalation hazards has not been measured, which will be pursued in the future by conducting a study with a diverse population of human subjects. We have also demonstrated the capabilities of the novel RPD to serve as an unobtrusive data acquisition platform for fit monitoring, which will be valuable for research and development of RPDs including understanding the human factors associated with the use of RPDs in real time and over time. By developing and demonstrating the design methodology based on the taxonomy of landmarks for the customization of RPDs, we have laid the foundation for providing respiratory protection, and improved source control to the full spectrum of the public including children, for whom options for respiratory protection are currently limited.

ACKNOWLEDGEMENTS

Georgia Tech researchers acknowledge funding for this research from the U.S, Centers for Disease Control and Prevention under Broad Agency Announcement (75D301-20-R-68024) through contract number 75D30120C09567. The authors thank Carbon 3D for printing the SIL 30 prototypes from the digital prototypes developed at Georgia Tech. We thank the anonymous reviewers for their thoughtful comments on our manuscript.

DISCLAIMER

The findings and conclusions in this report are those of the authors and do not necessarily represent the official position of the National Institute for Occupational Safety and Health, Centers for Disease Control and Prevention. Mention of any company or product does not constitute endorsement by the National Institute for Occupational Safety and Health, Centers for Disease Control and Prevention.

REFERENCES

3M. (2024) Technical Datasheet: 3M™ Reusable Half Face Respirator 6000 Series, Retrieved from: https://multimedia.3m.com/

Ashby. (2008) The CES EduPack Database of Natural and Man-Made Materials, Version 1.0, *Granta Design*, Cambridge, UK, January 2008.

Carbon 3D. (2022) SIL 30, https://www.carbon3d.com/materials/sil-30, Accessed: June 18, 2022.

Carbon 3D. (2024) SIL 30 Technical Datasheet, Doc #106453-00 Rev F, January 5, 2024. Retrieved from: www.carbon3d.com.

Dow. (2022) SILASTIC™ 3D 3335 Liquid Silicone Rubber, https://www.dow.com/en-us/pdp.silastic-3-d-3335-liquid-silicone-rubber-lsr.4137603z.html?productCatalogFlag=1#overview, Accessed: June 18, 2022.

Elkem. (2019) Silicones 3D Flyer Industrial, https://www.elkem.com/silicones/brands/amsil/, Accessed: June 18, 2022.

Formlabs. (2022a) Elastic 50A, https://formlabs.com/materials/flexible-elastic/. Accessed: June 19, 2022.

Formlabs. (2022b) Elastic 80A, https://formlabs.com/materials/flexible-elastic/. Accessed: September 9, 2022.

Granta. (2020) Chart from CES EduPack, *ANSYS Granta*. 2019.

Matweb (2024a). Properties of Thermoplastic Polymer, https://www.matweb.com/search/DataSheet.aspx?MatGUID=3190cb436efb45c0a1b4e64adfe908dd, Retrieved from Matweb.com.

Matweb (2024b). Properties of Silicone Rubber, https://www.matweb.com/search/DataSheet.aspx?MatGUID=cbe7a469897a47eda563816c86a73520), Retrieved from Matweb.com.

National Academies of Science, Engineering, and Medicine. (2019) *Reusable Elastomeric Respirators in Health Care: Considerations for Routine and Surge Use*. Washington, DC: The National Academies Press. https://doi.org/10.17226/25275.

Park (2024a) Park S, Tian Y, Bergman M, Pollard J, Zhuang Z, Jayaraman S. (2024) Next-Generation Custom-Fit Reusable Respiratory Protective Device with Continuous Fit Monitoring–Part I: Custom Fit Design. Journal of the International Society for Respiratory Protection. 2024;41(1):22-37.

Park (2024b) Park S, Tian Y, Bergman M, Pollard J, Zhuang Z, Jayaraman S. (2024) Next-Generation Custom-Fit Reusable Respiratory Protective Device with Continuous Fit Monitoring–Part II: Continuous Fit Monitoring. Journal of the International Society for Respiratory Protection. 2024;41(1):38-56.

Smooth-On. (2020) “Shore hardness scale,” https://www.smooth-on.com/page/durometer-shore-hardness-scale/, Accessed: November 14, 2020.

Wiley (2024). “Physical, Thermal, and Mechanical Properties of Polymers. https://onlinelibrary.wiley.com/doi/pdf/10.1002/9781118950623.app1, Accessed: July 4, 2024.